J|A|C|S
ARTICLES
Published on Web 06/06/2006

Solid-State Acid−Base Interactions in Complexes of Heterocyclic Bases with Dicarboxylic Acids: Crystallography, Hydrogen Bond Analysis, and ^{15}N NMR Spectroscopy

Z. Jane Li,* Yuriy Abramov, Jon Bordner, Jason Leonard,[†] Ales Medek, and Andrew V. Trask[‡]

Contribution from Pfizer Global Research and Development, Pfizer Inc., Eastern Point Road, Groton, Connecticut 06340

Received July 18, 2005; E-mail: jane.li@pfizer.com

Abstract: A cancer candidate, compound **1**, is a weak base with two heterocyclic basic nitrogens and five hydrogen-bonding functional groups, and is sparingly soluble in water rendering it unsuitable for pharmaceutical development. The crystalline acid−base pairs of **1**, collectively termed solid acid−base complexes, provide significant increases in the solubility and bioavailability compared to the free base, **1**. Three dicarboxylic acid−base complexes, sesquisuccinate **2**, dimalonate **3**, and dimaleate **4**, show the most favorable physicochemical profiles and are studied in greater detail. The structural analyses of the three complexes using crystal structure and solid-state NMR reveal that the proton-transfer behavior in these organic acid−base complexes vary successively correlating with ΔpK_a. As a result, **2** is a neutral complex, **3** is a mixed ionic and zwitterionic complex and **4** is an ionic salt. The addition of the acidic components leads to maximized hydrogen bond interactions forming extended three-dimensional networks. Although structurally similar, the packing arrangements of the three complexes are considerably different due to the presence of multiple functional groups and the flexible backbone of **1**. The findings in this study provide insight into the structural characteristics of complexes involving heterocyclic bases and carboxylic acids, and demonstrate that X-ray crystallography and ^{15}N solid-state NMR are truly complementary in elucidating hydrogen bonding interactions and the degree of proton transfer of these complexes.

Introduction

During drug discovery of a new chemical entity (NCE), there are often limitations in terms of solubility, stability and bioavailability for a single organic molecule. One of the effective ways to modify an NCE to improve its pharmaceutical profile is to explore a wider range of possible pharmaceutical compositions as the active pharmaceutical ingredients (API) without altering covalent bonding. Modifications that may help achieve desirable pharmaceutical properties include ionic complexes (salts) and neutral complexes (sometimes termed cocrystals). The diversity of multicomponent crystalline pharmaceutical solids not only improves performance and functionality of drug candidates but also enhances new compositional matter and the competitive edge in development.[1−6] Furthermore, a better understanding of the solid-state interactions in these complexes may lead to a rational design of crystalline API solid to rapidly advance a drug candidate through development to the launch of a product.

Because of diverse functional groups in drug molecules, the design and control of crystalline API solids often presents significant challenges. The most common multiple-component systems of APIs are ionized acid−base pairs, or salts. By definition, salt formation involves a proton transfer from the acidic moiety to the basic moiety, forming ionic components of opposite charges. However, many organic basic groups are weak bases and many organic acids are weak acids due to their inherent molecular composition and charge distribution. In addition, more than one basic or acidic group may be present, which naturally creates competition between these functional groups. As a result of competition, cooperation and balance between different intermolecular forces in a multicomponent system, an acid−base pair may not necessarily constitute a salt due to either partial or absent proton transfer. Lack of proton-transfer results in a crystalline complex that contains two or more different neutral molecular species, and is named a cocrystal.[7] However, the term cocrystal has been the subject of

[†] Current address: Franklin Pierce Law Center, Concord, NH 03301.
[‡] Current address: Pfizer Institute for Pharmaceutical Materials Science, Department of Chemistry, University of Cambridge, Lensfield Road, Cambridge, CB2 1EW, United Kingdom.

(1) Walsh, R. D. B.; Bradner, M. W.; Fleischman, S.; Morales, L. A.; Moulton, B.; Rodriguez-Hornedo, N.; Zaworotko, M. J. *Chem. Commun.* **2003**, 186−187.
(2) Remenar, J. F.; Morissette, S. L.; Peterson, M. L.; Moulton, B.; MacPhee, J. M.; Guzman, H. R.; Almarsson, Ö. *J. Am. Chem. Soc.* **2003**, *125*, 8456−8457.
(3) Fleischman, S. G.; Kuduva, S. S.; McMahon, J. A.; Moulton, B.; Bailey Walsh, R. D.; Rodriguez-Hornedo, N.; Zaworotko, M. J. *Cryst. Growth Des.* **2003**, *3*, 909−919.
(4) Childs, S. L.; Chyall, L. J.; Dunlap, J. T.; Smolenskaya, V. N.; Stahly, B. C.; Stahly, G. P. *J. Am. Chem. Soc.* **2004**, *126*, 13335−13342.
(5) Trask, A. V.; Motherwell, W. D. S.; Jones, W. *Cryst. Growth Des.* **2005**, *5*, 1013−1021.
(6) Sheth, A. R.; Lubach, J. W.; Munson, E. J.; Muller, F. X.; Grant, D. J. W. *J. Am. Chem. Soc.* **2005**, *127*, 6641−6651.

debate regarding its definition and use.[8,9] In the context of this research, the term "crystalline acid−base complex" (or simply "complex") is used to collectively include stoichiometric acid−base pairs regardless of proton transfer. The formula of a binary complex can be expressed as $m\boldsymbol{A}^{x-}\cdot n\boldsymbol{B}^{y+}$, where ***A*** and ***B*** denoted acid and base components, respectively, and *m*, *n*, *x*, and *y* can be any integers or fractions (*m*, *n* are not zero).

Compound **1** is a potent and selective ErbB2 inhibitor under development for the treatment of cancer.[10,11] However, the free base has serious limitations in solubility and bioavailability for drug delivery. Preparation of multicomponent API is the best option to enhance delivery profile.

Physicochemical properties including the melting point,[1] dissolution profile,[2,4] and physical stability[12,13] of pharmacologically active substances have been demonstrated recently to be subject to modification via complexation with organic molecules. The study of multicomponent organic crystalline complexes for the purpose of designing novel supramolecular materials has been the focus of research in recent years, and a number of literature reviews have been written on the subject.[14,15] However, most model molecules reported in the literature were either neutral or relatively rigid, and had relatively simple hydrogen bonding functionality. In contrast, compound **1**, as a cancer drug, is more complicated in its molecular structure with multiple basic sites and diverse hydrogen bonding functionalities. The variety of acid−base complexes of **1** exemplifies the complexity of organic acid−base interactions in the solid-state for pharmaceutical compounds.

In this study, the solid-state interactions of the acid−base complexes of **1** were investigated using crystal structural analysis, hydrogen bonding geometry and ^{15}N solid-state NMR to provide a detailed description of the acid−base interactions and to understand their impact on the physicochemical profiles of the multicomponent APIs. Solid-state ^{15}N NMR was particularly useful for studying heterocycles containing nitrogen in order to investigate the proton transfer and hydrogen bond strengths.[16,17] In the present work, complementary to X-ray diffraction, the sensitivity of the chemical shifts have been utilized to probe proton transfer and hydrogen bonding interactions.

Experimental Section

Preparation of Crystalline Complexes. Compound **1** is prepared according to the procedure as described previously.[10] The product was analyzed as **1** by elemental analysis and NMR spectra.

To a solution of **1** in hot THF/acetone (5/100), 2 equiv. of succinic acid were added. Crystals slowly formed as the solution cooled. After slurrying overnight, the product was isolated as a light yellow crystalline solid and verified as **2** by elemental analysis.

Two equivalents of malonic acid were added to a solution of **1** in hot acetone. As the solution cooled, crystals formed after 2 h, and the crystals were filtered after slurrying overnight. The light yellow solid was confirmed as **3** by elemental analysis.

A solution of maleic acid was prepared by dissolving 2.2 equiv. of maleic acid in 7:3 (v/v) chloroform/ethanol. Compound **1** was dissolved in the same solvent mixture, and added dropwise to the maleic acid solution with stirring. After about 2 days, white crystalline powder precipitated and was confirmed as **4** by elemental analysis.

Suitable single crystals of the compounds of interest were grown by slow evaporation from appropriate solvents.

Structural Determination. Crystals of suitable size were selected and mounted on a glass fiber. A representative crystal was surveyed and a 1 Å data set was collected at room temperature using Bruker diffractometers (Madison, Wisconsin) equipped with copper radiation and a graphite monochromator. Atomic scattering factors were taken from the International Tables for X-ray Crystallography.[18] Structures were obtained using direct methods. All necessary crystallographic computations and molecular displays were facilitated by the SHELXTL program provided by Bruker AXS, Inc.[19] Whenever possible, hydrogen positions were calculated; hydrogen positions on nitrogen or oxygen were located by difference maps.

Hydrogen-Bond Analysis. Mercury version 1.2.1 (distributed by CCDC, Cambridge, UK) was used to view hydrogen bond and hydrogen bond network. The hydrogen bond was identified by the maximum donor and acceptor distance of 3.2 Å with a minimum angle of D−H−A of 90°. Materials Studio version 3.1.0 by Accelrys (San Diego, CA) was also used to visualize the crystal packing and hydrogen bond network.

Solution NMR. The powder samples of **1** and its complexes (**2**, **3**, **4**) were dissolved in deuterated methanol. The solution spectra were collected at 298 K using a Bruker−Biospin 5 mm BBI probe on a Bruker-Biospin Advance NMR spectrometer (700 MHz ^{1}H frequency). The proton resonances were assigned using a suite of small-molecule solution NMR experiments including 1D proton and carbon spectra as well as 2D ^{1}H−^{13}C DEPTHSQC, BIRD−HMBC and ^{1}H−^{1}H COSY experiments. The proton chemical shifts were referenced using TMS at 0.00 ppm. The assignment of the nitrogen chemical shifts was based on the observation of long-range ^{1}H−^{15}N correlations using bilinear rotation decoupling filtered heteronuclear multiple bond correlation (**BIRD−HMBC**) experiment. The nitrogen chemical shifts were referenced indirectly to nitromethane at 0.00 ppm using an external sample of ^{15}N labeled DL-alanine setting its resonance to −313.3 ppm.

^{15}N Solid-State CPMAS NMR. Approximately 280 mg sample were tightly packed into a 7 mm ZrO spinner. One-dimensional ^{15}N spectra were collected at 295 K using ^{1}H−^{15}N cross-polarization magic angle spinning (**CPMAS**) on a Bruker-Biospin 7 mm BL CPMAS probe positioned into a wide-bore Bruker-Biospin Avance DSX NMR spectrometer operating at 11.74 T (500 MHz ^{1}H frequency). To minimize the intensities of the spinning sidebands, the samples were spun at 7.0 kHz corresponding to the maximum specified spinning speed for the 7 mm spinners.

To optimize the signal sensitivity, the cross-polarization contact time was adjusted to 2.5 ms, and the proton decoupling power was set to 65 kHz. The nitrogen spectra were acquired with approximately 10 000 scans, using a recycle delay of 8 s. The nitrogen chemical shifts were referenced indirectly to nitromethane at 0.00 ppm using an external solution sample of ^{15}N labeled DL-alanine setting its resonance to −313.3 ppm. To distinguish protonated and nonprotonated nitrogens, short contact-time CPMAS spectral editing experiment was employed

(7) Bernstein, J.; Etter, M. C.; Leiserowitz, L. In *Structure Correlation*; Burgi, H.-B., Dunitz, J. D., Eds.; VCH: Weinheim, 1994; Vol. 2, pp 431−507.
(8) Desiraju, G. R. *CrystEngComm* **2003**, *5*, 466−467.
(9) Dunitz, J. D. *CrystEngComm* **2003**, *5*, 506.
(10) Kath, J. C.; et al. *Abstr. Pap. Am. Chem. Soc.* **2003**, *226*, MEDI-012.
(11) Bhattacharya, S. K.; Cox, E. D.; Kath, J. C.; Mathiowetz, A. M.; Morris, J.; Moyer, J. D.; Pustilnik, L. R.; Rafidi, K.; Richter, D. T.; Su, C.; Wessel, M. D. *Biochem. Biophys. Res. Commun.* **2003**, *307*, 267−273.
(12) Trask, A. V.; Motherwell, W. D. S.; Jones, W. *Chem. Commun.* **2004**, 890−891.
(13) Jones, W. In *Organic Molecular Solids: Properties and Applications*; CRC Press: Boca Raton, 1997; pp 149−199.
(14) Aakeroy, C. B. *Acta Crystallogr., Sect. B: Struct. Commun.* **1997**, *B53*, 569−586.
(15) Lehn, J. M. *Angew. Chem., Int. Ed. Engl.* **1990**, *29*, 1304−1319.
(16) Foces-Foces, C.; Echevarria, A.; Jagerovic, N.; Alkorta, I.; Elguero, J.; Langer, U.; Klein, O.; Minguet-Bonvehi, M.; Limbach, H.-H. *J. Am. Chem. Soc.* **2001**, *123*, 7898−7906.
(17) Harris, R. K. *Solid State Sci.* **2004**, *6*, 1025−1037.
(18) Wilson, A. J. C. E. *International Tables for X-ray Crystallography*; Kluwer Academic: Dordrecht, The Netherlands, 1992; p 219, 500.
(19) *SHELXTL, Version 5.1*; Bruker AXS Inc., Analytical Systems: Madison, WI 53711, 1997.

Scheme 1. Molecular Structure of **1**, *E*-2-Methoxy-*N*-(3{4-[3-methyl-4-(6-methyl-pyridin-3-yloxyl)-phenylamino]-quinazolin-6-yl}-allyl)-acetamide: (a) the Atoms Involved in Hydrogen Bond Interactions Are Assigned as N1 to N5, O1B and O2B, Respectively, Used in the Discussion; (b) ORTEP Drawing of the Asymmetric Unit of **1**

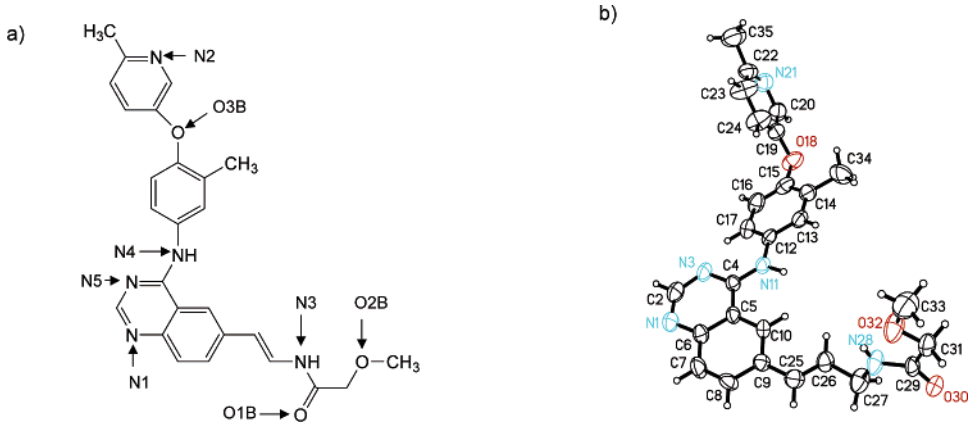

with the contact time limited to 120 μs. Only nitrogens experiencing a strong ^{1}H−^{15}N dipolar coupling (i.e., mostly nitrogens with directly attached protons) contributed to the observable signal. These assignments were further confirmed by a complementary spectral editing experiment of interrupted decoupling, whereby the proton decoupling field was turned-off for short period of 130 μs before acquisition to dephase signals originated from protonated nitrogens. This experiment was run with MAS rotation speed of only 3.5 kHz since the higher speed reduced the ^{1}H-^{15}N dipolar coupling and made the dephasing process inefficient.

DFT Calculations of ^{15}N Chemical Shifts. The Gaussian 03 program suite[20] was used to predict ^{15}N NMR shielding constants of **1** and **2** to support the ^{15}N assignments. The starting geometries of the free base and the sesquisuccinate including hydrogen bonds were taken from the single-crystal X-ray diffraction data. While the heavy atoms were fixed at the crystallographic positions, the hydrogen atoms were optimized at the B3LYP/3-21G* level of theory.[21,22] The ^{15}N isotropic shielding was calculated at the optimized geometries at the GIAO B3LYP/6-31G* level of theory.[23] The chemical shifts were calculated against the reference standard of the isotropic ^{15}N shielding of nitromethane computed at the same level.

Results and Discussion

The molecule of **1** contains several functional groups: acetamide, amine, quinazoline and methylpyridine. It has multiple hydrogen bond functional groups and two heterocyclic bases. To aid in the structural analysis, the nitrogen and oxygen atoms of **1** are assigned as shown in Scheme 1.

Compound **1**, a free base, has very low aqueous solubility and bioavailability, and cannot achieve the desired therapeutic efficacy. Its poor bioavailability is primarily due to a solubility limited absorption according to 'the rule of 5' proposed by Lipinski et al.[24] A salt screen using various pharmaceutically acceptable acidic counterions was conducted to search for potential salts (acid−base pairs) in order to improve the drug delivery profile. Among the twenty crystalline products of acid−base pairs,[25] the sesquisuccinate, the dimalonate and the dimaleate showed the most favorable overall physicochemical profiles and were considered for development.

Table 1. Comparison of the Overall Physicochemical Profiles

	compd			
	1 free base	**2** sesquisuccinate	**3** dimalonate	**4** dimaleate
stoichiometry (acid:base)	na	1.5:1	2:1	2:1
Δ pK_{a1} = pK_a(N1) − pK_{a1}(acid)	na	1.86	3.22	4.16
Δ pK_{a2} = pK_a(N2) − pK_{a1}(acid)	na	0.73	2.09	3.03
mp °C	167	143	161	173
aqueous solubility (μmol/mL)	0.0008	0.79	3.83	10.4

Table 1 summarizes the physicochemical profiles of the free base and three complexes. All of the crystalline complexes demonstrate a significant increase in solubility and bioavailability over **1**.

The pK_a values of the basic sites predicted by ACD/pK_a DB[26] are 6.2 for N1 and 4.9 for N2. The experimental pK_a values for the quinazoline amine N1 and the methyl-pyridine amine N2 are 6.1 and 4.9, respectively.[27] Succinic, malonic, and maleic acids have two carboxylic groups with different backbones and their pK_a values of the first ionizable carboxylic groups vary from relatively strong (maleic acid, pK_{a1} = 1.91) through intermediate (malonic acid, pK_{a1} = 2.85) to relatively weak (succinic acid, pK_{a1} = 4.21). Regardless of the acid strength, these three acid−base pairs demonstrate favorable physicochemical profiles as APIs, such as high melting, low-hygroscopicity, high aqueous solubility and acceptable stability, for solid dosage form development. It was proposed that these dicarboxylic acids form stable crystals with **1** because of their two carboxyl groups and the complementary geometry favorable for efficient packing.

Four crystal structures of **1**−**4** are selected for this study. The structural data are given in Table 2. To study the proton transfer and hydrogen bond formation, the packing diagrams of the crystal structures were analyzed using Mercury and Materials Studio. The hydrogen bond interactions are sum-

(20) Frisch, M. J.; et al. *Gaussian03, Revision B.04*, Gaussian Inc.: Wallingford, CT, 2004.
(21) Becke, A. D. *J. Chem. Phys.* **1993**, *98*, 5648−5652.
(22) Lee, C.; Yang, W.; Parr, R. G. *Phys. Rev. B* **1988**, *37*, 785−789.
(23) Wolinski, K.; Hinton, J. F.; Pulay, P. *J. Am. Chem. Soc.* **1990**, *112*, 8251−8260.
(24) Lipinski, C. A.; Lombardo, F.; Dominy, B. W.; Feeney, P. J. *Adv. Drug Delivery Rev.* **1997**, *23*, 3−25.
(25) Li, Z. J.; Leonard, J. A.; Trask, A. V.; Williams, G. R. Unpublished data, 2001.
(26) *ACD Lab, Version 4.56/26*; Advanced Chemical Development Inc.: Toronto, Canada, 2000.
(27) Yuhas, L.; Fiese, E. Unpublished data, 2002.

Table 2. Crystallographic Data

	1	2	3	4
empirical formula	$C_{27}H_{27}N_5O_3$	$C_{33}H_{39}N_5O_9$	$C_{33}H_{38}N_5O_{11}$	$C_{35}H_{38}N_5O_{11}$
formula weight	469.54	646.67	677.66	701.68
T, K	298(2)	298(2)	298(2)	298(2)
wavelength, Å	1.54178	1.54178	1.54178	1.54178
crystal system	monoclinic	monoclinic	monoclinic	triclinic
space group	*P*2(1)/*n*	*C*2/*c*	*P*2(1)/*c*	$P\bar{1}$
unit cell dimensions				
a, Å	9.4560(10)	29.1414(11)	12.0468(18)	4.7763(4)
b, Å	9.2370(10)	5.1132(2)	29.239(4)	19.0308(14)
c, Å	27.947(2)	44.2072(17)	9.9229(16)	19.1520(14)
α, deg	90	90	90	100.425(2)
β, deg	92.970(10)	103.6520(10)	114.241(5)	90.146(2)
γ, deg	90	90	90	95.269(2)
volume, Å^3	2437.8(3)	6401.0(4)	3187.0(8)	1704.6(2)
Z	4	8	4	2
calcd density, Mg/m^3	1.279	1.342	1.412	1.367
absorption coefficient, mm^{-1}	0.693	0.824	0.904	0.866
F(000)	992	2728	1424	736
crystal size, mm^3	0.24 × 0.08 × 0.06	0.02 × 0.14 × 0.18	0.02 × 0.04 × 0.04	0.03 × 0.04 × 0.20
reflections collected	2698	6386	6755	3709
independent reflections	2503 [*R*(int) = 0.0417]	2597 [*R*(int) = 0.0448]	2556 [*R*(int) = 0.0710]	2651 [*R*(int) = 0.1017]
refinement method, on F^2	full-matrix least-squares	full-matrix least-squares	full-matrix least-squares	full-matrix least-squares
data/restraints/parameters	2503/0/322	2597/5/446	2556/0/461	2651/0/476
goodness-of-fit on F^2	0.962	1.025	0.953	1.020
final *R* indices [$I > 2\sigma(I)$]	*R*1 = 0.06615	*R*1 = 0.0518	*R*1 = 0.0586	*R*1 = 0.0637
	w*R*2 = 0.1462	w*R*2 = 0.1357	w*R*2 = 0.1630	w*R*2 = 0.1698
largest diff. peak & hole, e Å^{-3}	0.234 and −0.226	0.387 and −0.269	0.384 and −0.309	0.212 and −0.236
extinction coefficient	none	0.00019(5)	0.0017(3)	0.0038(5)

Table 3. Summary of Hydrogen Bond Interactions (D and A denote donor and acceptor, respectively)

	compd			
	1	**2**	**3**	**4**
number of H-bond groups				
donor	2	5	6	6
acceptor	4	7	8	8
number of obsd H-bond				
intermolecular	1	5	6	5
intramolecular	1	1	1	2
total number of obsd H-bonds	2	6	7	7

Scheme 2. Proton Transfer between a Basic Nitrogen and a Hydroxyl of a Carboxylic Acid, Where *u*, *v*, and *w* Denote the Distances of N···H, O···H, and N···O, Respectively

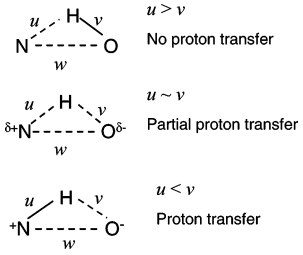

marized in Table 3; N5 and O3B are excluded as the hydrogen bond donor or acceptor since they are not involved in hydrogen bonding.

In all four structures, there are two more acceptors than donors and all donors are participating in hydrogen bonding.[28] The number of intermolecular hydrogen bonds is more than double in the complexes compared to that of the free base since the acidic components possess both strong hydrogen bond donors and acceptors that extend the hydrogen bond network in the crystal lattice.

Hydrogen Bond Geometry. Hydrogen bonding is one of the major cohesive forces in many organic crystals and has diverse geometry.[7,29] The characteristics of hydrogen bonds are one of the most intriguing aspects in these complexes. Scheme 2 demonstrates the variation of charge distribution and geometry in three proton transfer states. The partial proton transfer can be characterized by a pseudo-symmetric geometry with similar *u* and *υ*, and a shortened *w*, a contraction of N···O distance.

Table 4 lists the detailed geometry of the intermolecular hydrogen bond of **1**−**4** based on the crystallographic data. For the hydrogen bonds associated with the basic nitrogens, the changes of *u*, *υ*, and *w* corresponding to Scheme 2 are observed. Two D···A distances of **3***b* and **3***f* (∼2.545Å) are significantly shorter than the average distances of intermolecular hydrogen bonds (the average values are 2.85 Å for N···O and 2.65 Å for O···O).[31,32] These short D···A distances coincide with similar distances of N···H and O···H, which are greater than the average bond lengths of N−H and O−H, respectively. This type of hydrogen bond corresponds to a partial proton transfer or zwitterion structure in Scheme 2, in which the proton is shared to form very strong intermolecular hydrogen bonds.

The strength of hydrogen bonds depends on the geometry of hydrogen bonds and the donor−acceptor pairs. Due to the limitation of X-ray diffraction in the accuracy of hydrogen positions, the distances of N···O and O···O are more reliable and useful in hydrogen bond analysis.[30] Attempts to evaluate the relative strength of hydrogen bonds have been made using D···A distances as one of the numerical guiding values for general classifications.[32,33] For a constant donor−acceptor pair,

(28) Etter, M. C. *Acc. Chem. Res.* **1990**, *23*, 120−126.
(29) Pauling, L. *The Hydrogen Bond*; Cornell University Press: Ithaca, NY, 1960.
(30) Taylor, R.; Kennard, O. *Acc. Chem. Res.* **1984**, *17*, 320−326.
(31) Taylor, R.; Kennard, O. *Acta Crystallogr., Sect. B: Struct. Commun.* **1983**, *B39*, 133−138.
(32) Steiner, T. *Angew. Chem., Int. Ed.* **2002**, *41*, 48−76.

Table 4. Intermolecular Hydrogen Bond Geometry

H-bond name[a]	D···A[b]	hydrogen bond geometry D–H[c] (Å)	H···A (Å)	D···A (Å)	D – H···A (deg)
		1 − Free base			
d	N4H−O1B	0.930	2.072	2.990	169.3
		2 − Sesquisuccinate			
a	N1−C3OH	0.974	1.680	2.637	166.4
b	N2−C2OH	0.882	1.819	2.699	174.5
c	N3H−C3O1	0.970	2.073	2.962	151.4
d	N4H−C1O1	0.872	2.152	3.005	165.6
e	O1B−C1OH	0.833	1.814	2.631	166.4
		3 − Dimalonate			
a	N1H−C3O1	0.959	1.681	2.637	174.5
b	N2H−C1O2	1.120	1.431	**2.545**	172.0
c	N3H−C3O2	0.954	1.954	2.852	156.1
d	N4H−C1O1	0.829	2.531	3.166	134.3
e	O1B−C4OH	1.183	1.516	2.699	178.1
f	C3O1−C2OH	1.277	1.274	**2.545**	172.2
		4 − Dimaleate			
a	N1H−C3O1	0.956	1.775	2.731	178.3
b	N2H−C1O1	1.028	1.867	2.790	147.6
b2	N2H−C1O2	1.028	2.278	3.196	147.9
c	N3H−O1B	0.854	1.924	2.768	169.3
d	N4H−C2O1	0.936	1.931	2.854	168.0

[a] To facilitate the discussion, letter designations, *a*, *b*, *c*, *d*, and *e* are given to each hydrogen bond associated with N1, N2, N3, N4, and O1B, respectively; *f* is the hydrogen bond between two malonic acids. [b] For dicarboxylic acids, the carbons in first carboxylic group are labeled with C1 and C2, and for the second acid with C3 and C4; the hydroxyl group is labeled as OH and the carbonyl oxygen atoms of COO^- group is assigned O1 and O2, respectively. [c] The average NH length by X-ray is 0.938 Å (shorter than 1.030 Å determined by neutron diffraction) with typical random errors of 0.05−0.1 Å.[30]

intermolecular hydrogen bond strengths can be compared directly, with increasing D···A distance correlating to deceasing hydrogen bond strength. For the N···O donor and acceptor pairs involving the basic nitrogens in **2** to **4**, the rank order of D···A distances suggests the H-bond strength in an order of **3***b* > **3***a* ∼ **2***a* > **2***b* > **4***a* > **4***b*. In the next section, the ^{15}N solid-state NMR analysis provides further support for the rank order dividing into two groups, with and without proton transfer.

On the basis of the hydrogen bonding analyses, **2** and **3** possess several strong intermolecular hydrogen bonds, where the best acceptors of the base, N1, N2 and O1B, and the best donors of hydroxyl hydrogen from the carboxylic acids pair up. The intermolecular hydrogen bond interactions of **4** are not as strong as those in **2** and **3**, indicating that the ionic characters play more dominant roles for N1 and N2.

Structural Analysis. The multiple hydrogen bond functional groups of the base and the acids coupled with inherent flexibility of **1** leads to the complicated hydrogen bonding networks of the complexes, consisting of interlinked chains or rings in three-dimensional space. The differences in the acid backbone, although small, also play a role in hydrogen bonding and packing. Among these four crystal structures the hydrogen bond networks are different in terms of donor and acceptor pairs and geometry, suggesting interplay of molecular geometry, charge, hydrogen bond functional groups, and intermolecular interactions in the solids.

To compare the conformations of the base in **1**−**4**, the quinazoline ring is used as the anchor position shown in Figure

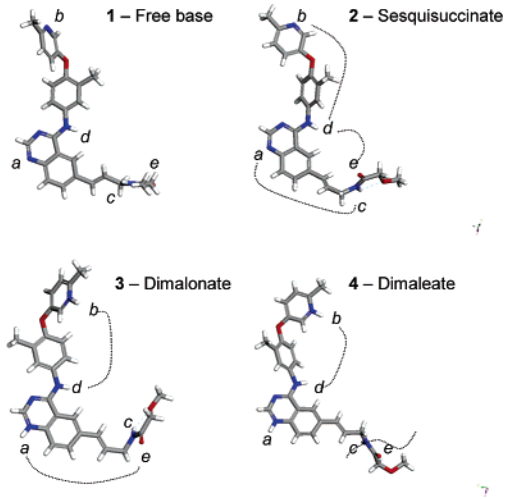

Figure 1. Conformation of the base in **1**−**4**: *a*, *b*, *c*, *d*, and *e* are hydrogen bonds involving N1 to N4 and O1B, respectively; the dot lines indicate the second-order intermolecular hydrogen bond networks given in the graph set analysis (Table 5).

1. The base molecule generally has a pseudo L-shape with a longer arm of three aromatic rings linked by an ether and amine, and a shorter arm of an alkene and an acetamide. Each arm has hydrogen bond functional groups pointing in different directions facilitating the formation of three-dimensional hydrogen bond networks. The acids are usually separated by the base, with an exception of **3** where two acids are hydrogen bonded through a shared hydrogen. To examine the similarity and difference in hydrogen bonds, graph set analysis is used.[28,34] Table 5 provides the graph set analysis of the hydrogen bond networks of **1**−**4**.

In graph set analysis, the single type of hydrogen bond is termed a motif. All hydrogen bond motifs are between acid and base except C(4) between amide groups of two bases in **4** and the hydrogen bond **3***f* between two malonic acids. Although there are many possible binary sets or second level networks, only the basic binary sets that are the shortest path involving two hydrogen bonds are given in Table 5. Multiple higher order networks exist by connecting to the third or fourth hydrogen bonds in the three-dimensional network but most of them are too complex and convoluted to provide direct and meaningful information. Two examples of higher order networks in **3** are given since they present some obvious features of the packing arrangements.

The graph set analysis reveals interesting features of hydrogen bonds in the 2nd order networks. Some common hydrogen bonding connectivity is observed, such as *ac* in **2** and **3**, and *bd* in all three complexes. Although there is similarity in the connectivity, such as *ac* and *bd*, the geometries of hydrogen bond pattern are different. For example, the network involving *bd* is a dimer ring of R(34) for **2** and **4** but a zigzag chain of C(14) for **3**, and the *ac* network forms a helical chain in **2** and a zigzag chain in **3**. The 34-membered rings of R(34) in **2** and **4** have different packing arrangements; in **2** it links with infinite chains while in **4** the ring stands alone. Apparently, the base as shown in Figure 1 dictates the hydrogen bond connectivity in the basic binary sets. Overall, the structures of higher order networks exhibit a wide variety of patterns as different chains and rings interlink in the crystal lattice and the following section provides more detailed analyses.

(33) Jeffrey, G. A. *An Introduction to Hydrogen Bonding*; Oxford University Press: New York, 1997.

Table 5. Graph Set Analysis[a] of the Hydrogen Bond Networks

compd	motif[b]	network[c]	pattern	packing
1	$S(5)\ R_2^2(24)$		dimer ring	stacked rings
2	S(5)*a, b, c, d, e*	$C_2^2(28) = ac$	helical chain	interconnected
		$R_4^4(34) = bd$	dimer ring	helical chains and
		$C_2^2(16) = de$	helical chain	cyclic dimers
3	S(5) *a, b, c, d, e, f*	$C_2^2(14) = ac$	zigzag chain	interconnected
		$C_2^2(14) = bd$	zigzag chain	chains and dimer
		$R_4^4(20) = cf$	dimer ring	rings in layers
		$C_3^3(19) = abd$*	zigzag chain	
		$R_5^5(28) = acadf$*	staircase ring	
4	S(7), *C*(4), *a, b, d*	$R_4^4(34) = bd$	dimer ring	stacked and interconnected rings

[a] Use of the graph set approach to analysis of hydrogen bond patterns reduces complicated hydrogen bond networks into combinations of simple patterns as chain, ring, intramolecular hydrogen bond, and other finite pattern, each specified as a designator of C, R, S (for self), and D, respectively. The graph set description is then given as $G_d^a(n)$ where G is one of the four possible designators, *d* and *a* are the number of donors and acceptors, and *n* is the number of the atoms. [b] The hydrogen bonds of *a*, *b*, *c*, *d*, *e*, and *f* described in Table 4 are the finite set, D, as motifs. [c] The networks are the selected 2nd order networks, i.e., the basic binary set, and the higher order hydrogen bond networks are denoted with asterisk.

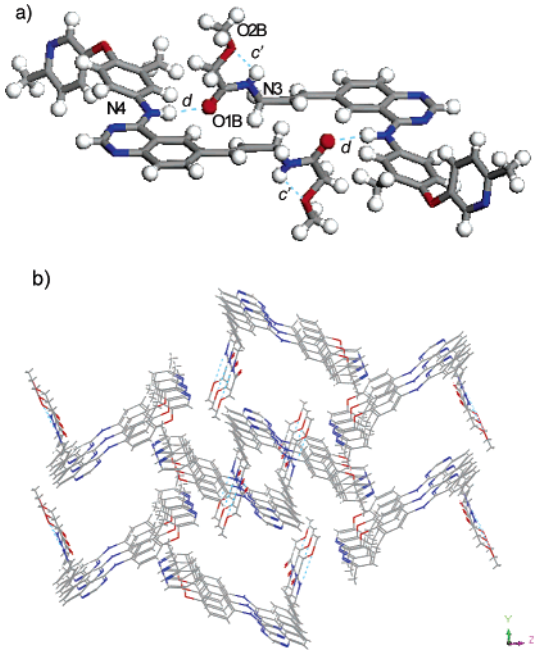

Figure 2. Crystal structure of **1**: (a) hydrogen bond dimer, and (b) the packing diagram view along *x* axis, where blue dash lines indicate hydrogen bonds, where *c*′ is the intramolecular H-bonds of the amide group N3H···O2B.

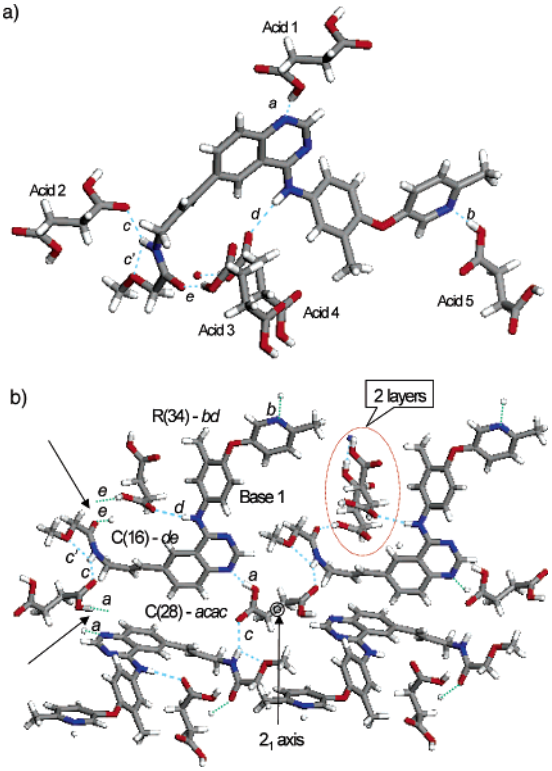

Figure 3. Crystal structure of **2**: (a) hydrogen bonds of one base to five acids, and (b) hydrogen bond network with the acid with a 2_1 axis as the center point to the plane; each quadrant has a R(34), a C(16) and a half of C(28) with the arrows pointed to the helical chains.

The structure of **1** has the least number of hydrogen bonds with one intramolecular hydrogen bond of the acetamide group, N3H···O2B, and only one intermolecular hydrogen bond between the amine N4H and the carbonyl oxygen O1B (Figure 2a). Although quinazoline N1 and pyridine N2 are strong acceptors, there is no hydrogen bonding interaction due to limited number of donors and geometric constraints in the solid-state. Two free base molecules are connected through a dimer ring R(24) through N4H of one base and O1B of the second base. The crystal structure of **1** (Figure 2b) is composed of the stacked dimers, thus the van der Waals interactions are dominant, which results in the very low aqueous solubility of the free base.

By X-ray diffraction, there is no proton transfer to N1 or N2 from the succinic acids, thus **2** is a neutral acid−base complex with a stoichiometry of one free base molecule to one and a half succinic acids. Figure 3a shows the individual hydrogen bonds where one base molecule is hydrogen bonded with five succinic acids through the acceptors O1B, N1, and N2 and the donor of N3 and N4. An addition of succinic acids in 1.5 molar ratios allows the hydrogen bonding of all donors and acceptors of the freebase. The packing diagram of **2** displays infinite hydrogen bond networks that can be visualized using the acid with 2-fold axis as the center point (Figure 3b). Through N1 and N3 of **1**, there is a helical hydrogen-bond chain of C(28) of *acac*. Adjacent to C(28), connecting N4 and O1B of **1** at the upper left quadrant, a second helical chain of 16-membered C(16), *de*, exists. These helical chains connect bases and acids

in different layers. The hydrogen bonds of *b* and *d* in the same base form a dimer ring of R(34), *bdbd*, with the neighboring pair of acid and base molecules. In Figure 3b, there are two helical chains of C(28), four helical chains of C(16), and four rings of R(34). The structure of **2** demonstrates the maximized hydrogen bond interactions of all donors and acceptors into infinite three- dimensional networks.

The dimalonate **3** has not only intricate hydrogen bond networks such as **2** but also a partial charge transfer. The partial proton transfer was first suggested by the relatively short N2H···O distance of **3***b*, 1.431 Å, less than the expected range of 1.5−2.2 Å for a relatively strong hydrogen bond, shown in Figure 4a.[35,36] Additional evidence came from the apparent longer distance of $N2^{+}$−H bond, 1.120 Å compared to the average N−H bond distance of 1.009 Å.[37] The more reliable distance from X-ray diffraction is O···N distance, 2.545 Å, which falls within the critical O···N distance at which a hydrogen bonded proton was found to be shared in a crystallographic study on a model system using variable temperature single-crystal neutron diffraction.[38,39] Together, these data suggest that the hydrogen atom in the pyridine nitrogen and carbonyl oxygen, $N2^{+}$−H···O2−C3, is shared between the donor and acceptor, producing a structure with a partially transferred proton or a resonance structure, $N^{\delta+}$···H···$O^{\delta-}$ like a zwitterion. Therefore, **3** is a mixed ionic and zwitterion complex as $\boldsymbol{A}^{-}\boldsymbol{A}^{\delta-}\cdot\boldsymbol{B}^{+\delta+}$, which cannot be fully described with either the "salt" or "cocrystal" term. Another interesting hydrogen bond **3***f* between two malonic acids has similar D···A distance of 2.545 Å as **3***b*. By the same reasoning as above, there is a shared hydrogen between the hydroxyl and the carbonyl groups from two acids, C4−$O^{\delta+}$···H···$O1^{\delta-}$−C1, in this case the hydrogen is located almost equidistance between the two oxygen atoms. Figure 4b,c shows a higher order hydrogen bond network and the layered packing diagram. Unlike **2**, the packing of **3** displays distinct hydrophilic and hydrophobic layers.

Two proton transfers occur in **4** from one of the carboxylic acids of each maleic acid to one base molecule N1 and N2. Although the protonated nitrogens are also hydrogen bonded to carbonyl oxygen, the hydrogen bonds, **4***a* and **4***b*, are not as strong as those in **2** and **3** based on the D···A distance analysis, suggesting ionic interaction may be more dominant in **4**. Both maleic acids are intramolecular H-bonded by the cis configuration of two carboxylic groups. Two base molecules and four maleic acids in antiparallel orientation form a large dimer of ring R(34) with extended chains of quinazoline and acetamide (Figure 5a). Another important hydrogen bond is the chain of the amide N3 and O1B of the base extends the hydrogen bond network in perpendicular to the dimer rings (Figure 5b). Compared to **2** and **3**, the packing of **4** has relatively simple and well-defined hydrogen bonds perpendicular to the dimer rings (Figure 5b).

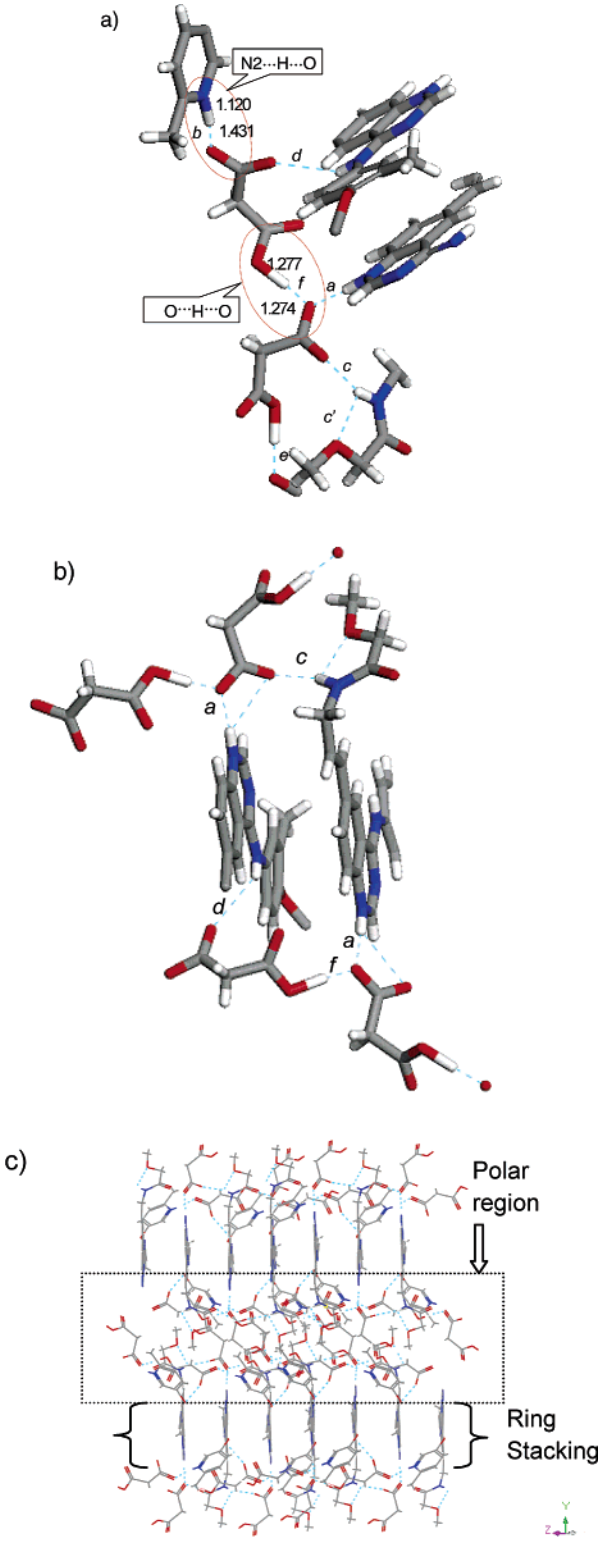

Figure 4. Crystal structure of **3**: (a) hydrogen bonds with shared hydrogens, on the top − **3***b*, a N2···O2, 2.544 Å; and in the middle − **3***f*, a 2.545 Å distance between O···O, (b) ring of R(28) − *acadf*, (c) packing diagram with alternating polar and nonpolar layers.

On the basis of the crystal structural analysis, it was found that **2** is a neutral complex, **3** is a mixed salt and zwitterionic complex, and **4** is a divalent salt. Apparently the differences in pK_a or ionization potential in solution transfer directly to the solids. This observation corroborates with the literature report that ionization or salt formation is observed when ΔpK_a is

(34) Bernstein, J.; Davis, R. E. *NATO ASI Ser., Ser. E* **1999**, *360*, 275−290.
(35) Desiraju, G.; Steiner, T. *The Weak Hydrogen Bond in Structural Chemistry and Biology*; Oxford University Press: Oxford, UK, 1999.
(36) Gilli, G.; Gilli, P. *J. Mol. Struct.* **2000**, *552*, 1−15.
(37) Orpen, A. G.; Brammer, L.; Allen, F. H.; Kennard, O.; Watson, D. G.; Taylor, R. In *Structure Correlation*; Burgi, H.-B., Dunitz, J. D., Eds.; VCH: Weinheim, 1994; Vol. 2, pp 751−858.
(38) Steiner, T.; Wilson, C. C.; Majerz, I. *Chem. Commun.* **2000**, 1231−1232.
(39) Steiner, T.; Majerz, I.; Wilson, C. C. *Angew. Chem., Int. Ed.* **2001**, *40*, 2651−2654.

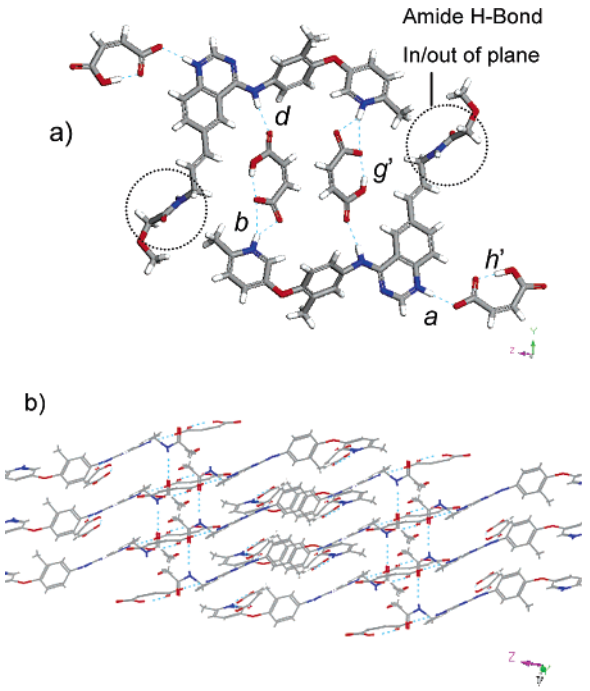

Figure 5. Crystal structure of **4**: (a) dimer ring R(34), and (b) the packing diagram with amide N−H···O chain C(4) perpendicular to the ring, where *g*′ and *h*′ are the intramolecular hydrogen bonds of the maleic acids.

greater than 2.[40] The key finding from the structural analysis is that there may exist a transition zone with ΔpK_a between 2 and 3 where a zwitterion may exist. The pK_a differences between many organic bases and acids are marginal with a value of less than 3, therefore, a partial to no proton transfer may actually occur in these acid−base pairs in the solid-state more often than has been realized. In these cases, it is necessary to analyze the hydrogen bond structures in detail to evaluate the proton transfer.

The diversity of chemical functions of **1** provides many possibilities for organic acid−base interactions, particularly ionization and hydrogen bond formation. Although a number of acid−base pairs of **1** with a variety of acids, either salts or neutral complexes, were prepared, only the dicarboxylic acids with complementarities for optimizing the hydrogen bonding produced the most stable crystalline complexes, **2**−**4**, with most favorable physicochemical properties. In these complexes, the acids with two carboxylic acid groups allowed optimal hydrogen bonding and intermolecular interactions leading to the formation of the stable crystalline complexes.

Furthermore, due to the specific hydrogen bonding interactions, the polymorph formation of these three complexes becomes limited, since no polymorphs were found in polymorph screens.[41] In this respect, there might be a potential advantage in control of the crystal form of multicomponent APIs in large-scale production. However, these multicomponent APIs of organic acid−base pairs showed a propensity to precipitate crystalline free base hydrate in aqueous solution when the pH of the solution is high.

The structural analysis reveals striking differences in the intermolecular interactions between the free base, which are dominated by nonpolar interactions, and the complexes, which are balanced between nonpolar and polar interactions. An addition of the acids plays dual roles in improving API properties, facilitating the formation of hydrogen bond networks in stabilizing the crystal lattice, and enhancing the aqueous solubility by lowering the pH of the solution that subsequently improves the bioavailability.

It has been proposed that understanding of hydrogen bond patterns will aid in the prediction of crystal structures for structurally similar compounds.[42,43] In these three complexes, it is observed that (1) the heterometric hydrogen bonds prevail, (2) the basic binary hydrogen bond networks show similar connectivity but different geometries, and (3) the overall packing of the three complexes are different in many respects despite the small difference in acid backbones. These results demonstrate, although it may be possible to rationalize local H-bond networks, there are significant challenges in the structure prediction of the multicomponent crystals.

^{15}N Assignments in Solid-State NMR. As discussed in the previous section, hydrogen bond structures naturally involve hydrogen atoms; however, the positions of hydrogen atoms in crystalline molecular compounds may not be precisely determined by routine X-ray diffraction.[31] Although neutron diffraction can produce higher precision data, it is not routinely accessible. With the advancement of solid-state NMR techniques, the chemical shifts of proton, carbon and nitrogen combined with quantum mechanical computation of chemical shielding can readily provide valuable information on inter- and intra-bond distance for structural elucidation.[17,44]

A study of proton-transfer involving basic nitrogens using ^{15}N solid-state NMR has been reported.[45] The ^{15}N chemical shifts of 1:1 complexes of a 2,4,6-trimethyl pyridine (collidine) and acids depended on the distances of A···H and D···A for ^{15}N labeled collidine with a series of structurally related carboxylic acids. It was suggested that the correlation observed in this simple system could be used to evaluate hydrogen bond geometry in more complicated systems.

The crystal structures of organic solids are often unavailable due to the difficulty in growing good quality single crystals for structural solution. ^{15}N solid-state NMR, using crystalline powder samples, could be particularly useful for investigating proton transfers in such cases since many drug molecules contain basic nitrogens in heterocyclic components. The availability of four crystal structures in this study offers an excellent opportunity to test the correlation between the chemical shift and proton transfer of the free base and the three complexes, and to further investigate hydrogen bonding and proton transfer.

The ^{15}N solid-state NMR study of **1**, the free base, and its complexes faced significant challenges because of the presence of five nitrogen atoms, while enrichment with ^{15}N isotope was not feasible from the synthesis point of view. Despite the low natural abundance of ^{15}N (0.368%), the optimized ^{15}N solid-state NMR spectra of these samples showed sufficient nitrogen sensitivity.

(40) Serajuddin, A. T.; Pudipeddi, M. *Salt-Selection Strategies*; Wiley-VCH: Weinheim, Germany, 2001; pp 135−160.
(41) Li, Z. J.; Trask, A. V.; Yuhas, L. Unpublished data, 2002.
(42) Gavezzotti, A. *J. Mol. Struct.* **2002**, *615*, 5−12.
(43) Aakeröy Christer, B.; Beatty Alicia, M.; Helfrich Brian, A. *J. Am. Chem. Soc.* **2002**, *124*, 14425−14432.
(44) Aliev, A. E.; Harris, K. D. M. *Struct. Bonding (Berlin, Germany)* **2004**, *108*, 1−53.
(45) Lorente, P.; Shenderovich, I. G.; Golubev, N. S.; Denisov, G. S.; Buntkowsky, G.; Limbach, H.-H. *Magn. Reson. Chem.* **2001**, *39*, S18−S29.

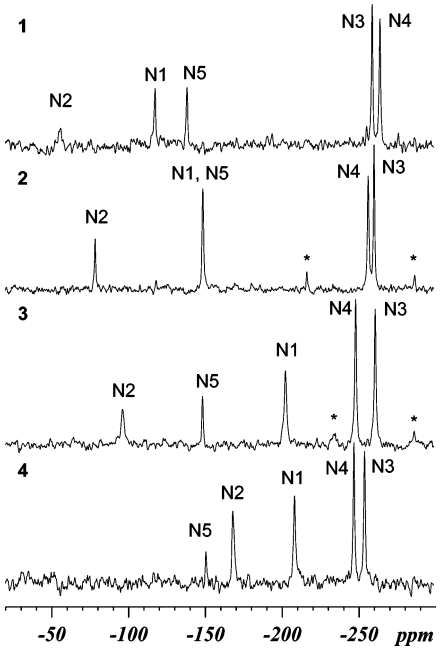

Figure 6. CPMAS ^{15}N NMR spectra of **1**−**4**; the assignments can be found in Table 6, the asterisks indicate the spinning sidebands; N2 peak in **1** was only observed with a shift of radio frequency close to N2 resonance; the peak assigned to N1 and N5 in **2** is of relatively higher intensity compared to other heterocyclic nitrogens.

Emsley et al.[46] reported nitrogen assignments of small peptides at natural ^{15}N abundance by employing 2D solid-state ^{1}H−^{15}N correlation experiments. In this study, obtaining 2D ^{1}H−^{15}N spectra with adequate sensitivity on **1** was hampered by the rather long proton longitudinal relaxation times. In the absence of the 2D correlations, the assignments of solid-state spectra are typically accomplished by combination of the solid state spectral editing and solution data. The solution nitrogen chemical shifts are assigned by the observation of long-range HMBC correlations to previously assigned proton resonances.

In this work, the solid-state 1D ^{15}N resonances are assigned based on the solution assignments, 1D solid-state spectral editing, calculated chemical shifts and information inferred from the single-crystal X-ray structures. The ^{15}N solid-state NMR spectra of **1**−**4** are shown in Figure 6 and the ^{15}N chemical shifts are given in Table 6.

Five nitrogen resonances were observed in the 1D ^{15}N CPMAS spectra of **1**, **3** and **4**, corresponding to the five nitrogen atoms in the base, but only four peaks were observed in **2**. For **1**, the rather broad peak at −56.1 ppm was initially absent and detected after shifting the nitrogen irradiation frequency closer to this peak's resonance. The resulting sensitivity enhancement of this peak is most likely due an improved spin-locking efficiency. The chemical shifts of **1** in the solid-state can be readily assigned following the same rank order in solution since relatively small differences are observed.

For **2**, only four peaks were observed. Assuming adequate sensitivity, the absence of a nitrogen peak could, in general, be due to a chemical exchange induced line broadening, or a peak overlap. The possibility of chemical exchange was ruled out since the spectrum acquired at 100 °C did not show any extra peak over the room temperature spectrum. Thus, a possibility of overlap of N1 and N5 peaks was proposed. The relatively high intensity of the peak at −149 ppm and small difference between N1 and N5 in solution (6.2 ppm) implied the high probability of overlapping. Further evidence came from the calculated ^{15}N shifts that predicted a difference of only 1.5 ppm between N1 and N5. On the basis of these analyses, the chemical shift at −149 ppm is assigned to both N1 and N5 of **2**.

Similar to **1**, the rank-order of chemical shifts of **2** should remain unchanged, because of absence of proton transfer in **2** by the single-crystal X-ray structure and the small difference between solution and solid. Although the rank order of chemical shifts remains the same as in solution for **1** and **2**, the relative changes are different for N1 and N2 due to hydrogen bonding interactions (see differences in Table 6). Without hydrogen bonding for N1 and N2 in **1**, down- field shifts of 14.4 and 15.3 ppm compared to the solution are observed, which may reflect the differences of the solution and solid. Unlike **1**, N1 and N2 of **2** show 7.2 and 5.4 ppm upfield shifts between the solution and solid, which can be attributed to the strong hydrogen bond interactions, usually inducing small upfield shifts.[45]

To assign the nitrogens in **3** and **4**, a spectral editing experiment using short contact time CPMAS was employed to differentiate protonated and nonprotonated nitrogens. In this experiment, only nitrogen atoms experiencing a strong ^{1}H−^{15}N dipolar coupling (i.e., nitrogens with directly attached protons) contribute to the observable signal. In Figure 7, the ^{15}N short contact time CPMAS spectra verify that both N3 and N4 for **1**−**4** are attached to hydrogen. For **3**, one additional peak at −203.0 ppm is observed. On the basis of pK_a data, it is known that N1 is a stronger base than N2, and the solution chemical shift of N1 is 87.9 ppm upfield compared to N2. Therefore the peak at −203.0 ppm is assigned as N1. Evidently, the N2 peak of **3** is absent in the short contact time CPMAS, implying that N2 is not directly attached to a proton. For **4**, two additional peaks in the short contact time CPMAS spectrum at −208.9 and −168.6 ppm are observed. They can be readily assigned to N1 and N2, respectively. The remaining peak of **4** at −151.0 ppm must be N5.

With the confirmation of the three nitrogen atoms of **3**, the two remaining unassigned nitrogen peaks at −148.8 and −96.5 ppm are to be assigned to N2 and N5. In **1**, **2**, and **4**, the N5 nitrogen shows chemical shift at −138.7, −149.0, and −151.0 ppm, respectively. From the single-crystal structures of **1**−**4**, it is known that N5 is not involved in protonation and hydrogen bonding. This nitrogen also shows only small differences between the solution and solid chemical shifts. Thus, the peak at −148.8 ppm for dimalonate should be N5, and the last remaining peak at −96.5 ppm is assigned to N2.

To verify the nitrogen assignments of **1** and **2**, calculations of nitrogen shielding constants were performed. The primary interest for the calculation was to validate the proposed overlapping resonances of N1 and N5 of **2**, and **1** was used as a reference to evaluate the accuracy of the calculated chemical shifts. The shielding constants are sensitive to both molecular geometry and environment,[47] thus hydrogen bond interactions were taken into consideration. For **1**, the hydrogen-bonded dimer was used in the computation (Figure 2a). To include the multiple

(46) Lesage, A.; Emsley, L. *J. Magn. Reson.* **2001**, *148*, 449−454.

(47) Facelli, J. C. *Calculations of Chemical Shieldings: Theory and Applications*; Wiley Interscience: New York, 2004; Vol. 20A, pp 42−69.

Table 6. ^{15}N Chemical Shift Assignments

	1			2			3			4		
atom	solution	solid	diff[a]	solution	solid	diff[a]	solution	solid	diff[a]	solution	solid	diff[a]
N4	−268.0	−264.8	3.2	−265.4	−257.0	8.4	−260.6	−248.9	11.7	−249.7	−247.7	2.0
N3	−262.0	−259.7	2.3	−261.1	−260.9	0.2	−262.2	−261.6	0.6	−262.6	−254.7	7.9
N5	−146.2	−138.7	7.5	−148.0	−149.0[b]	−1.0	−147.7	−148.8	−1.1	−149.4	−151.0	−1.6
N1	−132.2	−117.8	14.4	−141.8	−149.0[b]	−7.2	−161.4	−203.0	−41.6	−204.0	−208.9	−4.9
N2	−71.4	−56.1	15.3	−73.3	−78.7	−5.4	−73.5	−96.5	−23.0	−86.7	−168.6	−81.9

[a] Difference = solid − solution. [b] Only one peak was observed for N5 and N1 of **2**.

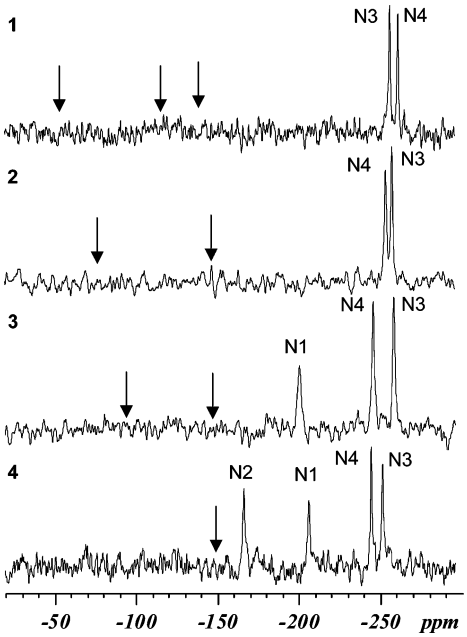

Figure 7. CPMAS ^{15}N NMR spectra of **1**−**4** with short contact time of 120 μs, only the nitrogens attached to protons were observed, the arrows point to the absent peaks compared to those in Figure 6.

hydrogen bonds in **2**, the computations were performed using a cluster with one base and five succinic acids (Figure 3a) with a total of 132 atoms. The calculated chemical shifts are shown in Table 7. Given the relatively large size of the clusters, the moderate basis set, B3LYP/6-31G* was used in computations. Despite the relatively modest level of the calculation, the predicted chemical shifts are in a good agreement with the experimental values, in terms of the correct order and small differences. The accuracy of the computations depends on many factors such as the precision of hydrogen position and the interaction of the neighboring atoms. Errors observed in these calculations are within the acceptable range in comparison to the literature reported data about 10−30 ppm.[48]

For **1**, a good agreement between the experimental and calculated values was observed. In fact, the N2 signal (initially missing due to inadequate sensitivity) was originally proposed to be −57 ppm based on Δppm of 14.4 ppm between solution and solid for N1 (Table 6), and the calculated value of −64.3 ppm was obtained simultaneously with the experimentally observed broad N2 peak by shifting the irradiation frequency. In **2**, the small calculated difference of 1.5 ppm strongly supports the overlapping of N1 and N5 signals in the experimental spectrum.

Table 7. Calculated Isotropic Chemical Shifts (in ppm)

	1			2		
atom	expt.	calc.	diff.[a]	expt.	calc.	diff.[a]
N4	−264.8	−259.4	5.4	−257.0	−259.2	−2.2
N3	−259.7	−257.1	2.6	−260.9	−266.0	−5.1
N5	−138.7	−146.3	−7.6	−149.0	**−154.8**	−5.8
N1	−117.8	−119.9	−2.1	−149.0	**−153.3**	−4.3
N2	**−56.1**	**−64.3**	−8.2	−78.1	−93.0	−14.9

[a] Difference = calculated − experimental.

Table 8. Difference in ^{15}N Solid-State NMR Chemical Shifts[a]

	Δppm[1] (complex – free base)		
atom	2	3	4
N4	7.8	15.9	17.1
N3	−1.2	−1.9	5.0
N5	−10.3	−10.1	−12.3
N1	−31.2	**−85.2**	**−91.1**
N2	−22.6	−40.4	**−112.5**

[a] A negative Δppm indicates an upfield shift. The bold numbers represent upfield shift greater than 80 ppm.

The ^{15}N chemical shifts can be used to probe the protonation and hydrogen bonding by examining the differences between free and protonated species. Table 8 presents the differences in ^{15}N chemical shifts between the free base and the complexes. It is known that protonation of pyridine nitrogen such as N1 or N2 induces significant upfield shift of 80−100 ppm. Indeed, the three basic nitrogens, N1 of **3**, and N1 and N2 of **4**, with proton transfer determined by the crystal structures, show large upfield shifts of 80−120 ppm compared to the free base.

The differences for N1 and N2 of **2**, and N2 of **3** in the range of 20−40 ppm are much smaller than those of protonated nitrogens, but correlate well to typically strong hydrogen bonds. Among them, the largest difference of 40.4 ppm for N2 of **3** is indicative of very strong hydrogen bond and a partial proton transfer. This agrees well with the rationale of a partial proton transfer from the D···A distance data from X-ray diffraction. More importantly, the ^{15}N chemical shift data provide explicit information that the proton is not attached to N2 or not within the covalent bond distance. Examples of detailed hydrogen bond geometry studied by ^{1}H MAS NMR and H/D isotope effects have been reported but are outside the scope of this work.[46,49] Although the hydrogen location might not be precisely determined by X-ray diffraction, the ^{15}N chemical shift data validate the partial proton transfer and confirm the existence of a zwitterion in **3**.

X-ray and NMR Data Correlation. To further explore the relationships between physical properties, structures and ^{15}N chemical shifts, the data are collectively presented in Figures 8

(48) Smith, E. D. L.; Hammond, R. B.; Jones, M. J.; Roberts, K. J.; Mitchell, J. B. O.; Price, S. L.; Harris, R. K.; Apperley, D. C.; Cherryman, J. C.; Docherty, R. *J. Phys. Chem. B* **2001**, *105*, 5818−5826.

(49) Limbach, H.-H. *Encyc. Nucl. Magn. Reson.* **2002**, *9*, 520−531.

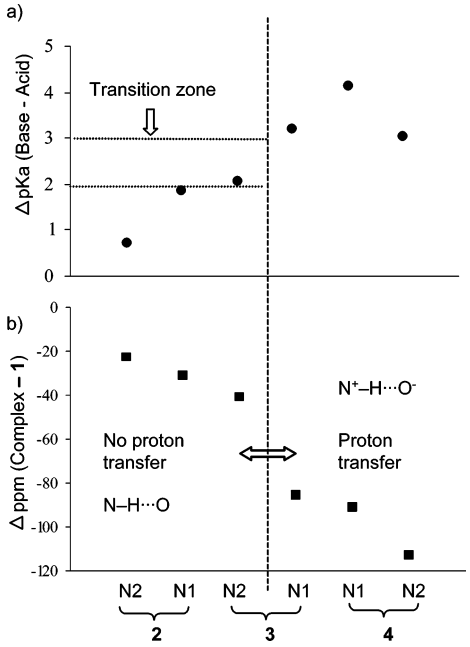

Figure 8. Correlations between chemical shifts and properties of the basic nitrogens: (a) ΔpK_a and (b) Δppm.

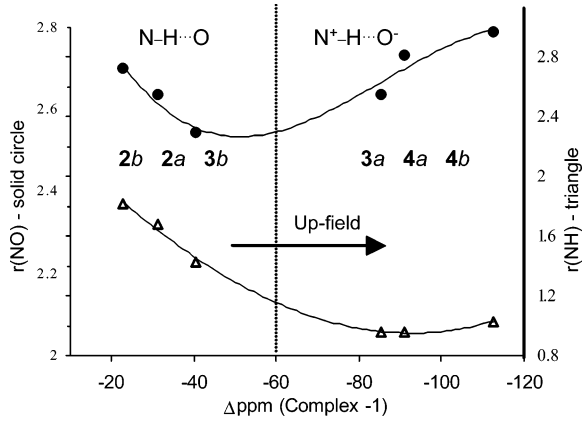

Figure 9. N−H and N···O distances as a function of the difference in ^{15}N chemical shifts − Δppm: the left half (Δppm of −20 to −60) − no proton transfer, and on the right (Δppm of −60 to −120) − proton transferred; the fitted lines display the trend of changes.

and 9. Since the proton transfer or ionization depends largely on the strength of the acidic components in these complexes, a correlation is observed between ΔpK_a values and Δppm. As shown in Figure 8, a minimum 3 units difference in pK_a values of the base and the acid is required for proton transfer for upfield shifts greater than 80 ppm. A transition zone with ΔpK_a of 2−3 may exist where the proton transfer is intermediate as discussed previously.

Figure 9 displays the distances of NH and NO as a function of the upfield ^{15}N chemical shifts (Δppm) of the basic nitrogens. A clear division between protonated and nonprotonated is observed despite a relatively small number of samples. This apparent separation between the protonated and nonprotonated nitrogens was demonstrated in a group of nine structurally related pyridine nitrogens from various plots of isotopic H/D effects against ^{15}N chemical shifts to correlate proton transfer.[45] It is noteworthy that the small (∼0.25 Å) changes in the N···O distances translate to large upfield chemical shift differences depending on proton transfer. For r(NO), the upfield shift is between 20 and 60 ppm, whereas for r(N^+O^-), it is greater than 80 ppm. The correlation shown in Figure 9 can be a useful tool for evaluating proton transfer in crystal acid−base complexes of heterocycles containing nitrogen.

The observed trends in Figure 9 also have corroborated with hydrogen bond analysis. On the left half, the upfield shift increases with contraction of the NO and NH distances, corresponding to the stronger hydrogen bond interactions. The right half, however, shows the opposite trends for the charged species, with a lesser degree of changes in the NH distances. The orders based on distances, **3***b*, **2***a*, **2***b* on the left and **3***a*, **4***a*, **4***b* on the right in both r(NO) and r(NH) along the trend lines agree with the relative strengths of hydrogen bonds based on D···A distance analysis in the order of **3***b* > **3***a* ∼ **2***a* > **2***b* > **4***a* > **4***b* (the underline indicates hydrogen bonds with proton transferred). Most importantly, the plot of distance and Δppm in Figure 9 provides valuable information to refine the D···A distance analysis into a direct comparison of the hydrogen bond strengths with or without proton transfer.

In summary, the correlations discussed above provide greater details of proton transfer and hydrogen bonding. For a heterocyclic basic nitrogen, an upfield shift of 80 ppm or greater is observed when a proton is transferred from a carboxylic acid to a heterocyclic base, and an upfield shift of 20 to 40 ppm is indicative of the strong hydrogen bond interactions, the greater the upfield shifts the stronger the hydrogen bonding interactions and the shorter the distance between nitrogen and hydrogen. The difference in chemical shifts (Δppm) of ^{15}N correlates very well with the hydrogen bond geometry analysis in assessing the hydrogen bond strength for the structural related complexes. Since organic bases with heterocyclic nitrogens are rather common in pharmaceutical compounds, the findings from this work may be applied to many other crystalline materials.

Conclusions

The three complexes of **1** and dicarboxylic acids have demonstrated successive proton transfer following ΔpK_a values of an acid−base pair, from a neutral complex of the sesquisuccinate to a mixed zwitterionic complex of the partial-proton transferred dimalonate to a divalent ionic dimaleate. Regardless of the degrees of proton transfer; these multicomponent APIs demonstrate significant advantages in their solubility and subsequently improved bioavailability compared to that of the free base for enhancing drug delivery profile.

Among **2**−**4**, while the hydrogen bond geometry and packing vary considerably, each achieved maximum hydrogen bonds by balancing the nonpolar and polar interactions and the ionization. The ^{15}N solid-state NMR technique proves to be a valuable tool for structural analysis of proton transfer and hydrogen bonding of heterocyclic bases by systematically correlating the changes in chemical shifts. It can be applied in the investigation of proton transfer in absence of the crystallographic data.

Overall, this study demonstrates the structural complexity of a drug candidate and its multicomponent APIs in pharmaceutical development. The combination of crystallography and ^{15}N solid-state NMR is particularly useful in elucidating the intricate crystal structures of nitrogen-containing heterocyclic molecules. The knowledge gained from the hydrogen bond networks provides insights in understanding and predicting the proton

transfer and hydrogen bonding networks of multicomponent APIs involving structurally similar molecular species and other organic acid−base complexes.

Acknowledgment. The authors would like to thank Neil Feeder for his consultation on crystal structural analysis; John Kath, Dan Richter, Joel Morris, and Carl Thompson for collaboration in synthetic chemistry and crystallization; Glenn Williams, Ivan Samardjiev, Mike Perlman, Maria Lopez, Ricardo Borjas, and Lisa Yuhas for their contributions on salt screen and analytical work; Linda Lohr and Andrew Jenson for their work on ^{15}N solution NMR; Stephen Anderson for helpful discussions and reviewing the manuscript; and Professor Robin Harris from University of Durham for his valuable suggestions on ^{15}N solid-state NMR.

Supporting Information Available: Crystallographic information of compound **1** to **4** as CIF files. The complete list of authors for the refs 10 and 20. This material is available free of charge via the Internet at http://pubs.acs.org.

JA0541332